Journal of GeoEngineering, Vol. 14, No. 2, pp. 85-96, June 2019
http://dx.doi.org/10.6310/jog.201906_14(2).4

STRENGTH AND COMPRESSIBILITY CHARACTERISTICS OF AMORPHOUS TROPICAL PEAT

Akeem Gbenga Amuda [1], Alsidqi Hasan [2*],
Dayang Norfaranina Datu Unoi [3], and Siti Noor Linda [4]

ABSTRACT

Peat is viewed to deflect from the standard guidelines of soil behaviours due to the influence of structural fibres and high compressibility. Hence, the laboratory strength behaviour of peat is often complex, and the geotechnical test results may be doubtful. Amorphous peat is expected to behave differently since the fibres have been broken down into smaller organic contents and humus material. Laboratory tests such as scanning electron microscopy (SEM), one-dimensional (1D) oedometer tests and isotropically consolidated undrained (CIUC) triaxial tests were conducted on amorphous peat samples obtained from a site in Kota-Samarahan, Malaysia. The microstructure of amorphous peat indicates colloidal amorphous-granular particles with no visible evidence of hollow cellular connections. The measured compressibility and strength properties reflect the effect of decomposition and are somewhat different from that of fibrous peat. Interestingly, the strain hardening characteristic which complicates the interpretation of strength results is less significant, and the tension cutoff line is not reached. Based on the outcome of this study, strength and settlement behaviour of amorphous peat can be reasonably measured in the laboratory for design and construction of highways, embankments and other infrastructures.

Key words: Amorphous peat, decomposition, shear strength, microstructure, compressibility, triaxial test.

1. INTRODUCTION

Peat material is majorly composed of organic content from remains of vegetation. It is viewed as one of the most complex geotechnical material due to its high compressibility properties and low strength characteristics as well as heterogeneous behaviour due to a different degree of organic decomposition (De-Guzman and Alfaro 2018; Mesri and Ajlouni 2007). Construction of infrastructures on peat often results in large settlement, long-term creep and sudden catastrophic failures (Boylan *et al.* 2011; Hendry *et al.* 2012). Malaysia falls in the tropical region where peat is found in abundance, and 70% of Malaysia peatlands is in Sarawak, Eastern part of Malaysia. This area coincides with various upcoming infrastructural development such as the Sarawak Corridor of Renewable Energy (SCORE) and the Pan Borneo Highway project (East Malaysia). There is a need to focus greater attention on understanding the properties and mechanical behaviour of peat to prevent unexpected failure and high maintenance of infrastructures. A lot of the research work on peat strength measurement has been carried out on fibrous peat in colder climatic regions. However, a comprehensive database on strength behaviour of amorphous tropical peat is required for adequate material models to aid effective design and construction of infrastructures on peat.

Peat ranges from highly fibrous to amorphous depending on the state and rate of decomposition of the organic content. The ASTM D4427 (2002) classifies peat with a fibre content of less than 20% as amorphous peat. During the period of peat decomposition, the physical plant structure diminishes, chemical state changes and fibres degenerate to smaller organic grains and become more or less equidimensional (Huat *et al.* 2003; Mesri and Ajlouni 2007; Pichan and O'Kelly 2012). The outcome of decomposition is that the fibre content reduces progressively and the hollow cell structures close up (Mesri and Ajlouni 2007). The rate at which peat changes in structure depends on the types of vegetation, climate, available microbes and anthropogenic activities such as farming and drainage control. Given these structural changes in fibre, the geotechnical characteristics of amorphous peat are expected to be different from that of fibrous peat; however extensive research is required to establish the differences (O'Kelly and Pichan 2013; Santagata *et al.* 2008). The microstructure and particle arrangements in peat also change with decomposition (Boelter 1968).

The knowledge of peat microstructure is as essential as the knowledge of material properties in inorganic soils (Hobbs 1986). Geotechnical engineers, more often than not, neglect the investigation of the microstructure for settlement prediction and stability analysis, maybe because it is believed that decomposition does not occur fast enough to change the microstructure within the design life of a geotechnical structure (Hobbs 1986; Pichan and O'Kelly 2012). At present, there is limited research correlating different peat microstructure to their physical and engineering properties (Huat *et al.* 2014).

Manuscript received May 31, 2018; revised November 7, 2018; accepted December 6, 2018.

[1] Lecturer, Department of Civil Engineering, Nile University of Nigeria, Abuja, Nigeria.
[2*] Senior Lecturer (corresponding author), Department of Civil Engineering, Universiti Malaysia, Sarawak, Malaysia (e-mail: halsidqi@unimas. my).
[3] Graduate student, Department of Civil Engineering, Universiti Malaysia, Sarawak, Malaysia.
[4] Associate Professor, Department of Civil Engineering, Universiti Malaysia, Sarawak, Malaysia.

The presence of fibre in peat increases compressibility, frictional resistance and induces anisotropy (Landva and Pheeney 1980; Mesri and Ajlouni 2007; Huat 2004). Fibrous peat in its natural form (horizontal orientation) exhibits large vertical strains and provides stiffness to stresses that are in an approximately vertical direction (Hendry *et al.* 2012; Landva and Pheeney 1980). Fibre generates tension and provides extra shearing resistance to stress in a perpendicular direction. Observations of in-situ peat and undisturbed samples have shown that the orientation of fibres in peat is predominantly horizontal in their natural deposition (Edil and Wang 2000; Hendry *et al.* 2012; Landva and Pheeney 1980; Yamaguchi *et al.* 1985b). However, highly decomposed (amorphous) peat may not be able to offer such additional resistance even in its natural deposition. Since the fibres in amorphous peat are broken down, amorphous peat will be more isotropic, less permeable, less compressible and possess lower friction angle (Mesri and Ajlouni 2007; Zhang and O'Kelly 2013). Therefore, it is understandable that the results of laboratory characterisation of peat will depend on the fibre content and orientation during testing (Hendry *et al.* 2012; Landva and La Rochelle 1983).

Triaxial testing is one of the most common laboratory tests for soil strength including peat. During triaxial testing, both the major and minor principal stress is controlled independently, and shear failure occurs as a result of differences in the principal stresses. The alignment of peat fibre is mostly perpendicular to the failure plane in the triaxial test, and it serves as reinforcement during triaxial testing. Hence, the strain hardening effect of the fibre during triaxial compression test may not allow for peak strength be reached (Long 2005). As a result, additional values of effective angle of friction should be expected. Lastly, for the undrained triaxial test type, the effective stress path of fibrous peat often reaches to the tension cut-off line, thereby interpreting test results becomes more complicated (Yamaguchi *et al.* 1985b; Den-Haan and Kruse 2006; Zwanenburg *et al.* 2012; Zwanenburg and Jardine 2015). Other apparatus such as ring shear and direct shear tests are not significantly affected by fibre because their shear direction is parallel to the fibre orientation (Zwanenburg *et al.* 2012). However, these devices have their limitations for peat testing, such as partial drainage and sample disturbance in direct shear and ring shear respectively (Amuda *et al.* 2019; Grognet 2011; AO Landva and La Rochelle 1983; O'Kelly 2015). The triaxial test remains a proper way of estimating the undrained shear strength of soil. Due to the additional angle of friction caused by fibre resistance in the triaxial test of peat, researchers have proposed different techniques to estimate the actual effective angle of friction for peat (Cola and Cortellazzo 2005; Hendry *et al.* 2012; Landva and La Rochelle 1983). For instance, Hendry *et al.* (2012) proposed that the effective angle of friction from the frictional relationship of peat particles alone can be estimated by extrapolating the linear portion of the strain hardening caused by fibre tension in the deviatoric stress *vs.* axial strain plot.

This paper presents geotechnical characteristics of amorphous tropical peat through the microstructure of peat via scanning electron micrographs, the strength behaviour via undrained triaxial testing of peat and the compressibility characteristics via one-dimensional oedometer tests.

2. DISTRIBUTION OF PEATLANDS IN SARAWAK, MALAYSIA AND STUDY AREA

Malaysia is one of the countries in the world with abundant peatlands, and about 70% of her peat land is found in the Sarawak region (about 17,000 km^2). Sarawak's peat has an average depth of 20 m, and it shrinks with time as draining processes continue which result in a high subsidence rate. Wösten *et al.* (1997) predicted a subsidence rate of 20 mm/year for peat in this region, which is the highest in the world (Al-Ani *et al.* 2013). Table 1 shows the estimates of the peat areas in Sarawak state with Sibu/Mukah division having the highest peatlands of about 6,000 km^2 and Kapit division has the lowest with about 21 km^2. This region falls in a tropical climate with steady rainfall and all year round high temperature that sustains formation and decomposition of peat. Hence, a significant percentage of peat in this area is moderate to highly decomposed, unlike temperate region with cold weather. Peat deposits in the tropics are rapidly decomposed because of the influence of easily penetrating air and the combination of considerable heat with humidity (Joosten 2016). Peats in the inland forest are more aerated and therefore more decomposed than those in the lowlands (coastal region) under strongly anaerobic conditions (Zulkifley *et al.* 2013). Distribution of peatlands in Sarawak together with the location of the field site where the samples used for this study is obtained is represented in Fig 1. The peat material used for this study is obtained from Kampung Endap, Kota Samarahan (KEP), Sarawak, Malaysia (1°25′37.2″N, 110°27′32.3″E). The study area is close to the coastal area, which is prone to high tide flooding (Zulkifley *et al.* 2014). Therefore, the water table in this region is always near the ground surface (about 0.3 m below the ground surface) with negligible fluctuation throughout the year (Habib-Musa 2015; Tie and Kueh 1979). The depth of peat in this area is about 6 m underlain by organic clay.

3. CLASSIFICATION OF PEAT

Wide variation exists in the classification of peat and organic soils due to differences in geographical locations and professional fields such as agriculture, botany, geology and engineering (Zulkifley *et al.* 2013). Peat and various organic soils are classified based on their organic content, fibre content, and decomposition. The organic content gives the percentage of the

Table 1 Estimates of peatlands areas in Sarawak (Wetlands International 2010)

Division	Total area of peat (km^2)
Sibu/Mukah	6,004
Sri aman/Betong	3,404
Miri	2,960
Kota samarahan	1,656
Sarikei	744
Bintulu	1,574
Limbang	347
Kuching	268
Kapit	21
Total	16,978

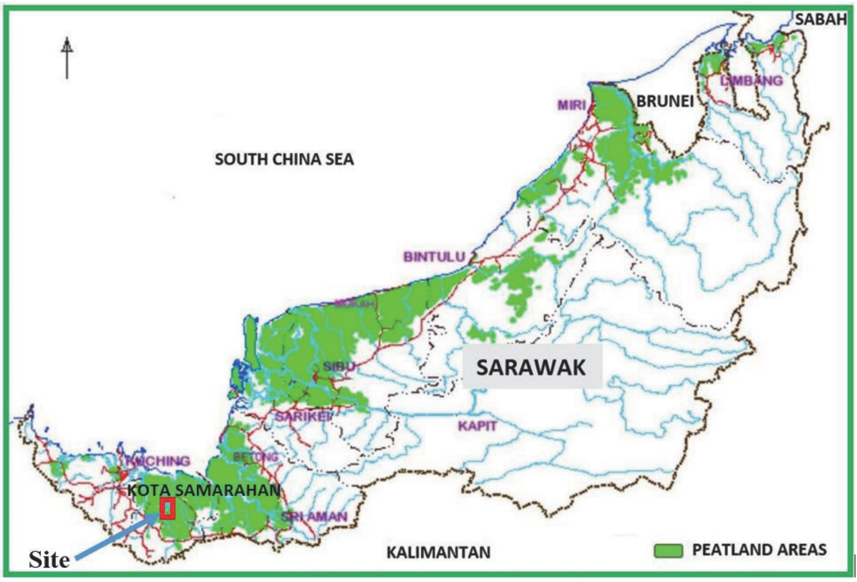

Fig. 1 Distribution of peatlands in Sarawak, Malaysia (DID Sarawak 2016)

organic-based material in soils, and fibre content is the degree of the organic substance that is yet to be humified. Peat is described as soils with organic contents higher than 35% by soil scientists. For geotechnical engineers, Landva *et al.* (1983) specified peat to have organic content above 80% from loss of ignition test, and Von post used the state of decomposition and wetness to classify peat into ten broad categories. The Unified Soil Classification System (USCS) combines all soils that are composed primarily of plant tissue in all stages of decomposition, colours and odour as peat (ASTM D2487 2011). The Public Works Department, Malaysia has improved the on the various existing classification works, by combining factors of organic content and degree of decomposition for a comprehensive classification of tropical peats (Zainorabidin and Wijeyesekera 2007; Zulkifley *et al.* 2013). Table 2 shows the Extended Malaysian Soil Classification System (MSCS) for peat.

4. SAMPLING AND INDEX PROPERTIES

The undisturbed samples were collected with thin-walled PVC sampler at 1.2 m depth. The PVC sampler measures 100 mm in external diameter and 150 mm in height with a cutting edge angle of 30°. The area ratio of the PVC tube used for undisturbed sampling is 10.8% with no clearance ratio, which is within the ASTM D1587/D1587M (2015) recommended ratios to minimise soil disturbance induced by soil displacement. The picture of the undisturbed sampling is presented in Fig. 2. The disturbed samples were collected by scooping method and put into plastic containers for reconstitution in the laboratory. The containers were sealed with silicone sealant to avoid disturbance and loss of moisture. Index tests were carried out on the peat samples, and the summary is presented in Table 3. Visual examination of the sample indicates a dark brown coloured organic material with a smooth texture. The von-Post squeeze test on the peat sample did not show any recognisable plant structure on the hand after squeezing out the peat paste in between fingers. Almost all peat escaped through the fingers except for few undecomposed fibres. The nearly complete decomposed peat is classified to be Von-Post index H8-H9 (Sapric).

The loss of ignition was measured in the laboratory by heating few peat samples at a temperature of 450°C until there was no significant change in mass (ASTM D2974 2014). The estimated loss of ignition ranges from 92% to 96%. Other peat samples were soaked in a dispersing agent (5% sodium hexametaphosphate) for 15 hours to determine the fibre content (ASTM D1997 2013). After the samples were washed through a No. 100 sieve, and oven-dried at 110 ± 5°C, the measured fibre content was within 3.5 to 6.2%. The specific gravity was determined using pycnometer tests (ASTM D854 2010) by using kerosene instead of distilled water. Note that kerosene was used instead of

Table 2 Malaysian soil classification systems (MSCS) for peat (Adapted from Zulkifley *et al.* 2013)

Soil group	Organic content	Group symbol	Subgroup symbol	Degree of humification	Subgroup name	Field identification
Peat	> 75%	Pt	Ptf	H1-H3	Fibric or fibrous	Dark brown to black in colour. Material has low density so seems light. Majority of mass is organic, so if peat is fibrous, the whole mass will be recognisable plant remains. If highly humified, the peat will be more likely to smell strongly.
			Pth	H4-H6	Hemic or moderately decomposed peat	
			Pta	H7-H10	Sapric or amorphous	

water because peat may be lighter than water. The measured specific gravity ranges from 1.69 ~ 1.71. The moisture content of peat was determined by oven-drying samples at a temperature of 80^0C until there was no further change in mass. The water content ranges from 378% to 620%.

Based on the index tests results in Table 3, the peat can be considered as highly humified with less fibre. Note that humus materials are the product of secondary synthesis of peat and are chemically active due to their small sizes and high electrical surface charge (Santagata *et al.* 2008). These humus materials are also referred to colloids of organic soils similar to fine clay in mineral soils because of their comparable chemical characteristics (Huat *et al.* 2014).

5. SAMPLE PREPARATION

Air drying technique was employed to remove the pore fluids of peat samples for use in SEM analysis. The sample was air dried at room temperature for two weeks instead of putting it in the oven at a high temperature. The air dry option is prefered, because heat may affect the microstructure of peat, which is from plant remains. The air-dried sample was pulverised using a rubber hammer and stored in an airtight polythene bag.

Fig. 2 Picture showing the undisturbed sampling method

Table 3 Index properties of Kampung Endap peat

Index properties	Value range	Technique and device
Von post	H8-H9	Hand squeezing
Organic content (%)	92 - 96	High-temperature oxidation method (ASTM D2974).
Fibre content (%)	3.5 - 6.2	Oven drying (ASTM D1997-91)
Moisture content (%)	378 - 620	Oven drying (ASTM D2216)
Specific gravity	1.69-1.71	Pycnometer using the kerosene (ASTM D854-02)
Liquid limit (%)	540 - 602	Fall cone (BS 1377-2)
Colour	Dark brown	Visual examination
Unified soil classification system	Pt	ASTM D2487

The reconstituted peat samples for use in oedometer and triaxial tests were prepared in the laboratory by hand mixing the disturbed samples obtained from the field. The hand mixed sample was pre-consolidated in 400 mm height cylinders as shown in Fig. 3(a) until primary consolidation has been achieved. One of the cylinders has an inside diameter of 38 mm (for triaxial test samples), and the second, 100 mm (for oedometer test samples). The pre-consolidation stress applied for each triaxial test samples in the steel cylinder was 5 kPa less than the isotropic consolidation pressure to be applied during the tests. Once the primary consolidation is reached, the pre-consolidated sample is extruded and trimmed into the required sample height for the triaxial testing. Figure 3(b) shows a pre-consolidated sample for the triaxial test. Each sample was carefully wrapped with polythene and kept in an airtight desiccator for preservation. The same procedure was followed for the preparation of reconstituted samples for oedometer tests, except that the samples were all pre-consolidated with 5 kPa vertical effective stress. The undisturbed samples were cut with the particular test mould from the undisturbed samples for the tests.

6. SCANNING ELECTRON MICROSCOPY (SEM)

The imaging of peat microstructure was carried out with the Hitachi TM 3000 Tabletop scanning electron microscopy to understand the morphology and spatial arrangement of the peat constituents. Figure 4 shows the setup of the electron microscope used for carrying out these investigations. The pulverised sample was sprinkled on a 5 mm aluminium stubs (sample holder). Before the sprinkling of the sample, the stubs are overlaid with double-sided carbon tape as a form of adhesive to gum the sample to the stubs. Then the sample was coated with a thin layer of gold in a sputtering diode system for 10 minutes. The gold coating is to allow repulsion of the scattered electron that hits the surface of the sample when it is placed into the Scanning Electron Microscopy (SEM) for observation. Various samples were prepared according to the explained method and examined with the SEM.

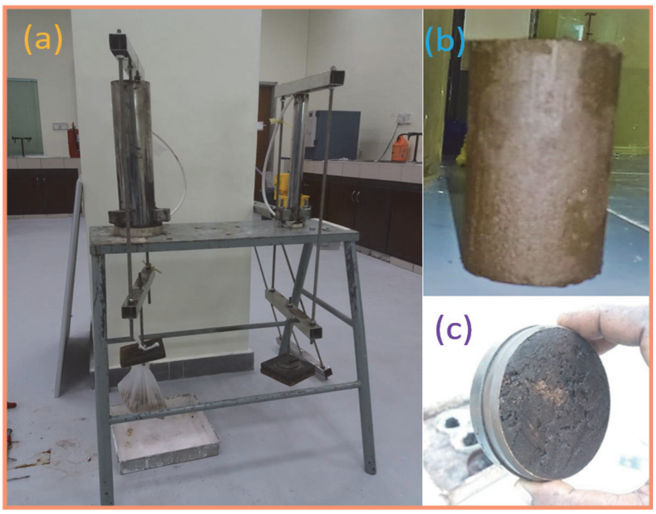

Fig. 3 (a) The pre-consolidation setup; (b) the pre-consolidated sample for the triaxial test; (c) the undisturbed sample with oedometer ring

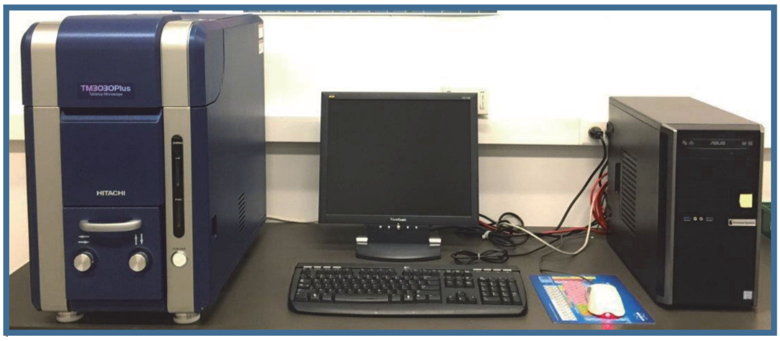

Fig. 4 Setup of Hitachi TM 3000 Tabletop scanning electron microscopy

Figures 5 and 6 present representative images from SEM micrographs of the peat samples that were taken at different magnifications. Majorly, the observed microstructure shows homogeneous non-crystalline micro-particles that are colloidal in structure and jelly-like in texture. Figures 5(a) to 5(c) are a different magnification of the same sample while Figs. 5(d) to 5(f) are also a different magnification of another sample. Looking at the higher magnifications (Figs. 5(c) and 5(f)), it is clear that the colloidal structure has no intra-assemblage pore space, but pore water bounds their surfaces. Peat with colloidal microstructure is referred to as amorphous granular material and are in the range of H8 to H10 in the Von Post and Granlund (1926) classification. Organic colloids are very small in size (less than 2μm) because it is formed from humified peat with fewer fibres (Huat *et al.* 2014; Kazemian *et al.* 2011).

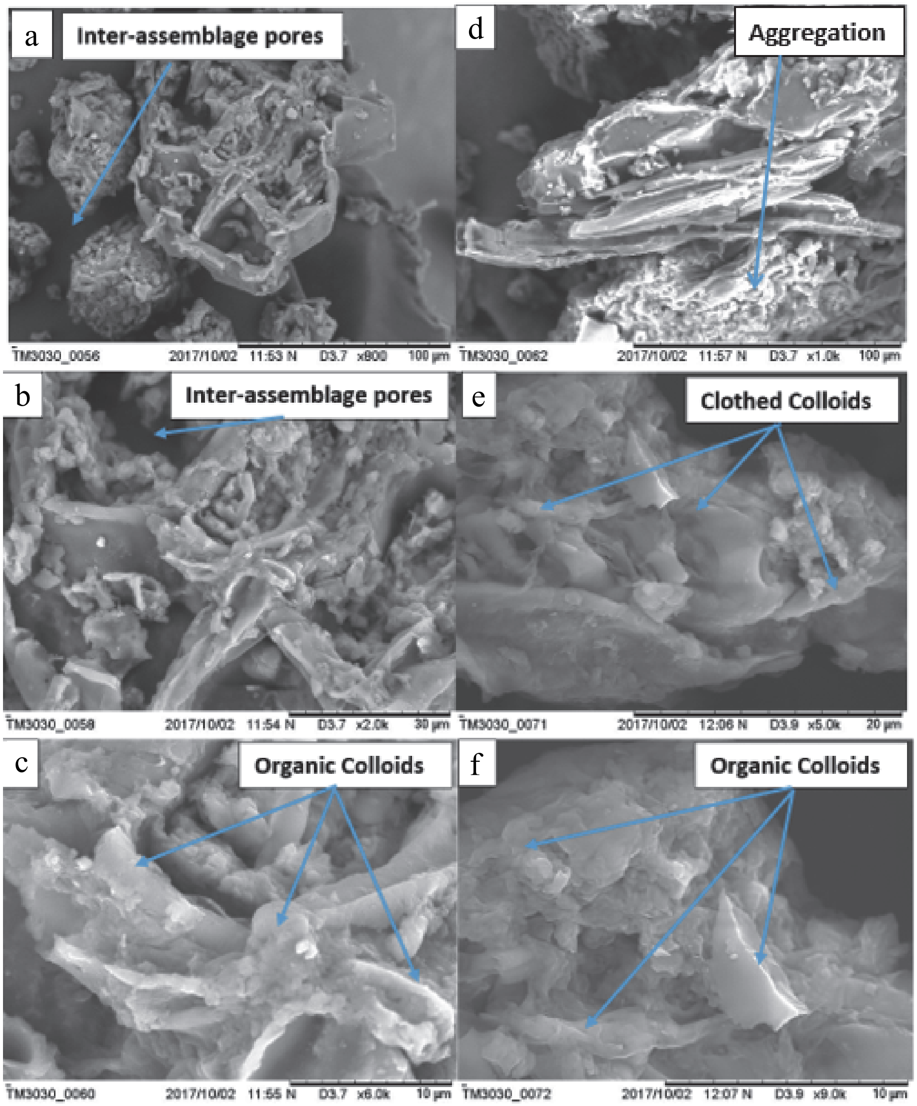

Fig. 5 Scanning electron micrograph of amorphous peat samples showing colloidal structures

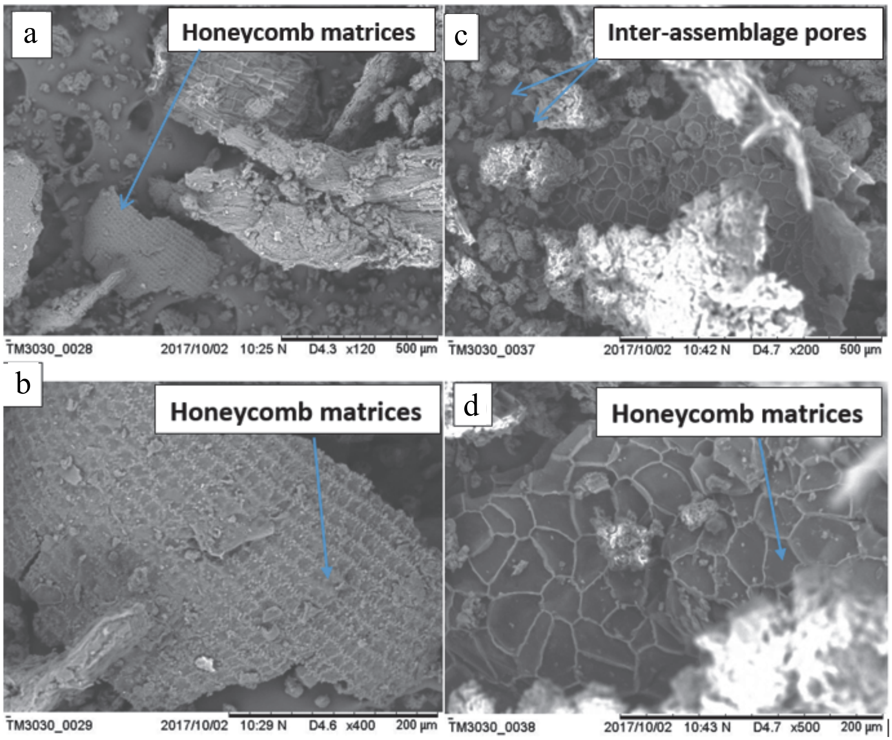

Fig. 6 Scanning electron micrograph of amorphous peat samples showing sheet-like structures

The second type of microstructure particles observed is sheet-like microstructure, existing in some of the samples investigated (Fig. 6). The microstructure appears in the form of honeycomb intra-assemblage with a solid intraparticle arrangement without any discernable water-holding cells or voids (Figs. 6(b) and 6(d)). The sheet-like particles have no direct contact with one another. It is also not possible to observe any distinct leaf structures, which means they are highly decomposed. Peat with sheet-like microstructure are mostly stemmed sheaths (integuments) and are classified as H7 organic materials (Landva 2007).

The SEM results complement the data of the index properties. The SEM micrograph shows that the hollow perforated cellular structure of fibrous peat has been lost. Hence the peat could become more gelatinous and compact, relatively high specific gravity (Hobbs 1986; Boylan 2008). It is also noted that there are no significant cavities for storage of water in the intraparticle spatial arrangement of the peat samples. Hence, water is stored mainly in between the interparticle voids only. Thus the moisture content is lower than that of fibrous peat (Haut *et al.* 2011). Note that two-thirds of the water content in fibrous peat are mostly stored within the hollow cellular fibres while one- third is stored in the interparticle voids between the fibres (Landva and Pheeney 1980; Mesri and Ajlouni 2007; O'Kelly 2014). Given that significant part of the fibre has been humified, the fibre content is also on the low side.

7. ONE-DIMENSIONAL COMPRESSION TESTS

One-dimensional tests were conducted using a conventional oedometer apparatus to observe the compressibility anisotropy of amorphous peat through the settlement behaviour of both undisturbed and reconstituted samples. The peat samples were cut with an oedometer ring with an inner diameter of 75 mm and height of 20 mm as shown in Fig 3(c). The inner side of the ring was lightly lubricated with silicon grease to reduce sidewall friction. The undisturbed samples were cut from the undisturbed sample while the reconstituted samples were cut from the 100 mm diameter pre-consolidated sample. Each sample was trimmed at both faces and placed into the assembled oedometer apparatus. Filter papers and porous stones were placed at the bottom and top of each sample before placing the top cap. After setting each sample in the apparatus, it was soaked in water for about 24 hours to allow full saturation before loading the sample for settlement observation. A series of load increments from 10, 20, 40, 80, and 160 kPa was used for the test, and the change in settlement for each load increment was recorded for 24 hours. Three samples each were tested for both the reconstituted and undisturbed tests in this study.

Figures 7(a) and 7(b) show the cumulative axial strain with elapsed time for each loading steps employed for both the reconstituted and undisturbed samples respectively. Three tests were conducted for each set of incremental load (10 to 160 kPa), and each test is represented with alphabet A, B, and C. The repeatability of the results is generally good as depicted in the two plots and both the reconstituted and undisturbed are somewhat identical. The reconstituted tests results are more consistent than the undisturbed samples. From the e-log(t) curves of the reconstituted samples, the axial strain for the first and last (10 kPa and 160 kPa) incremental loads is approximately 9.5% and 48% respectively, while that of the undisturbed sample is 9.7% and 53.1% respectively. The undisturbed amorphous peat samples are slightly more compressible than the reconstituted samples, although the initial settlement for both samples is high. The end-of-primary consolidation for each test was determined by the Casagrande's e-log(t) curve method. The duration of primary consolidation for the first two loadings

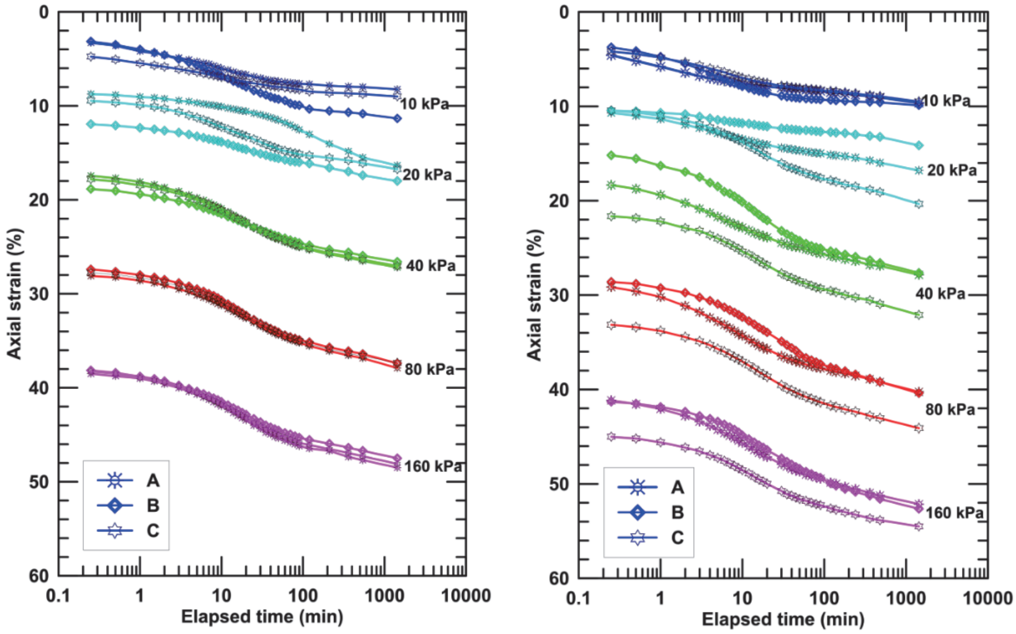

(a) Reconstituted samples (b) Undisturbed samples

Fig. 7 Axial strain from loading increments *vs.* elapsed time

in the undisturbed tests is relatively shorter than other tests because of the high initial permeability of the virgin peat deposit with high void ratio and expulsion of entrapped biogas (Mesri and Ajlouni 2007).

The compressibility curves (*e vs.* log of vertical effective stress, σ_v' plots) for all the amorphous peat samples tested in this study are shown in Fig. 8. The data are superimposed with test linear fit lines. All the *e*-log σ_v' plots converge with an increase in the vertical effective stress. The average compressibility and deformability parameters of amorphous peat estimated from this study are presented in Table 4. The compression index, C_c represents the slope of *e vs.* log σ_v' for each set of incremental loading test ($C_c = \Delta e/\Delta \log \sigma_v'$). The average C_c for the reconstituted and undisturbed tests are 4.4 and 5.4 respectively and are within the lower range of C_c for peat in the literature. The range of compression index of peat in the literature according to Huat *et al.* (2014) is within 2 to 15. Also, the difference between the values of C_c in the reconstituted and undisturbed samples less significant. The estimated C_c agrees with the empirical correlation of $C_c = w/100$ suggested by Mesri and Ajlouni (2007) for normally consolidated and fully saturated peat deposits. Recall that the estimated moisture content, *w* of the amorphous peat samples utilised in this study range from 378 to 620.

The deformability of amorphous peat particles was estimated from the ratios of C_α / C_c, where C_α is defined as the secondary compression index, and it is measured from the slope of the secondary consolidation line ($C_\alpha = \Delta e/\Delta \log t$). Note that the C_α changes with time for each level of σ_v' while C_c changes with only the σ_v'. Therefore, the rate of change in C_α with time is proportional to the rate of change in C_c with σ_v'. The estimated mean of C_α for each set of incremental loading ranges from 0.2 to 0.31, while the ratio of C_α / C_c is from 0.044 to 0.056 (see Table 4). Given the close range values of the ratio of C_α / C_c for the reconstituted and undisturbed sample, it can be said that compressibility and deformability anisotropy is lower in amorphous peat than that of fibrous peat. Lower deformability, permeability anisotropy is often reported for amorphous peat than fibrous peat (Lee *et al.* 2015; Mesri and Ajlouni 2007; Yamaguchi *et al.* 1985a; Yamaguchi *et al.* 1985b).

Table 4 Compressibility parameters of amorphous peat

Type of Tests	Tests	C_c	C_α	C_α / C_c
Reconstituted	A	4.48	0.24	0.054
	B	4.27	0.22	0.052
	C	4.38	0.2	0.046
Undisturbed	A	5.35	0.25	0.047
	B	5.45	0.24	0.044
	C	5.49	0.31	0.056

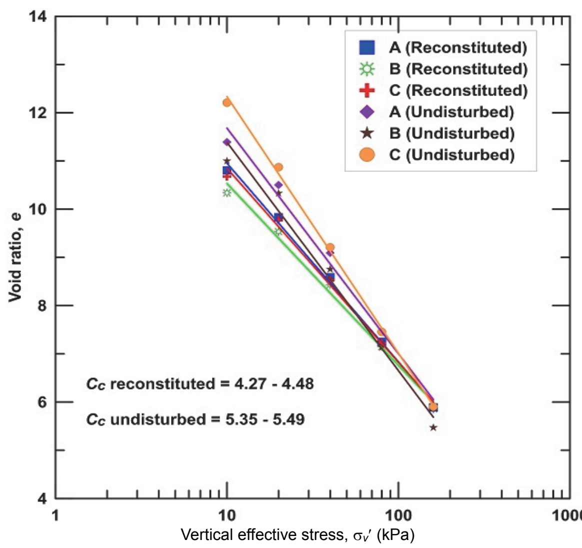

Fig. 8 Void ratio *vs.* vertical effective stress curves for both reconstituted and undisturbed samples

Figure 9 plots C_α *vs.* compression index, C_c for each effective stress level. It also includes data from the most relevant past reports, namely James Bay Peat, Middleton Peat and organic clay. Santagata *et al.* (2008) reported an average value of C_α / C_c to be 0.095, though some of the data are as high as 0.122. The author stated that the reason for high values of C_α / C_c is because most of the samples tested are high in fibre content. Mesri *et al.* (1997) also reported that the average relationship of C_α / C_c is 0.052 and 0.035 for amorphous peaty clay (Zhang and O'kelly 2013). Generally, a mean value of 0.06 ± 0.01 has been reported for peat and mean value of 0.04 ± 0.01 for organic clay without fibre (Santagata *et al.* 2008; Mesri and Ajlouni 2007). The average C_α / C_c results obtained from this study is 0.056 with some of the data as low as 0.041. Based on the reviewed works of literature and Fig. 9, we propose that the value of C_α / C_c might decrease with the decomposition of peat.

8. CONSOLIDATED UNDRAINED (CIUC) TRIAXIAL TEST

Undrained triaxial tests were performed on reconstituted samples to establish the strength behaviour of amorphous peat in triaxial test. It was not possible to trim and place the undisturbed sample collected for the undisturbed triaxial test without disturbance because the sample kept deforming during the trimming process. The in-situ effective stress of the samples obtained at 1 m depth below the surface is very low, and the sample deforms under own weight even when the sample was collected with a 38 mm diameter PVC tube (Hayashi *et al.* 2012). Hence undisturbed triaxial test is not included in this study. The test was conducted with an automated CIUC apparatus with a LoadTrac-II and two FlowTrac-II systems manufactured by Geocomp Corporation (Geocomp triaxial manual 2013). The picture of the automated triaxial system is shown in Fig. 10. One of the FlowTrac-II controls the cell pressure and volume while the other one controls the sample pressure (back pressure) and volume. Before the placement of sample on the pedestal, the sample is underlaid with a filter paper and porous stone (of the same diameter with the sample). Each sample was then carefully placed on the triaxial pedestal. Another set of filter paper and porous stone is placed at the top end of the sample. The sample is enclosed with a rubber membrane by a membrane fitting tool to reduce sample disturbance (for low effective stress peat sample) during preparation and installation. Hard Gabo "O" ring seals were used to fasten the upper and lower ends of the rubber membrane against the top cap and the pedestal respectively before the cylindrical chamber is used to cover it.

The chamber surrounding the sample was then filled with distilled water and placed on the automated Geocomp triaxial testing machine. Once the sample is in place on the Geocomp triaxial machine and all the required test conditions are selected, the system automatically runs the entire test from saturation to consolidation and shearing without the intervention of the operator. Hence the back pressure, Skempton's *B*-value, consolidation pressure and strain rate were input into the machine at once before the test started. A back pressure adequate to remove all the air (100 kPa) was applied to all the peat sample throughout the consolidation and undrained shear stage. The *B*-value was set to ≥ 0.95 for full sample saturation check. Once the desired *B*-value is reached, the test moves to the consolidation stage. The machine automatically stops consolidation when the time to end of primary consolidation, t_{100} is reached, then the test moves on to the shearing stage. Each of the samples was isotropically consolidated to various consolidation pressure ranging from 10, 20, 30, 50, and 100 kPa.

Faster strain rate in a constant strain rate triaxial test increases the measured strength (Hanrahan 1954; Boylan 2008). In this test, the strain rate was estimated by dividing the estimated failure strain (15%) by 10 t_{50} (where t_{50} is the time required to achieve 50% consolidation). The estimated strain rate used for all the triaxial tests is 0.18%/hr to allow for full equalisation of shear-induced pore water pressure within the sample. The membrane stiffness correction, q_m is calculated using Eq. (1) (ASTM D4767 2011).

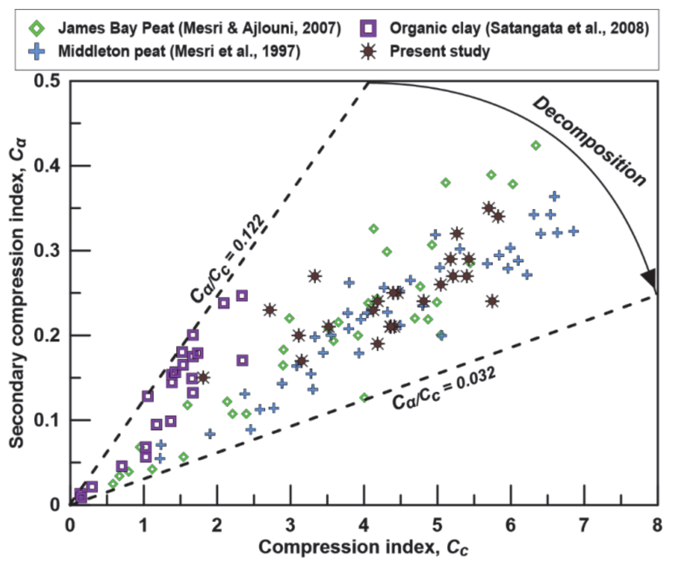

Fig. 9 Secondary compression index (C_α) *vs.* compression index (C_c) for peats

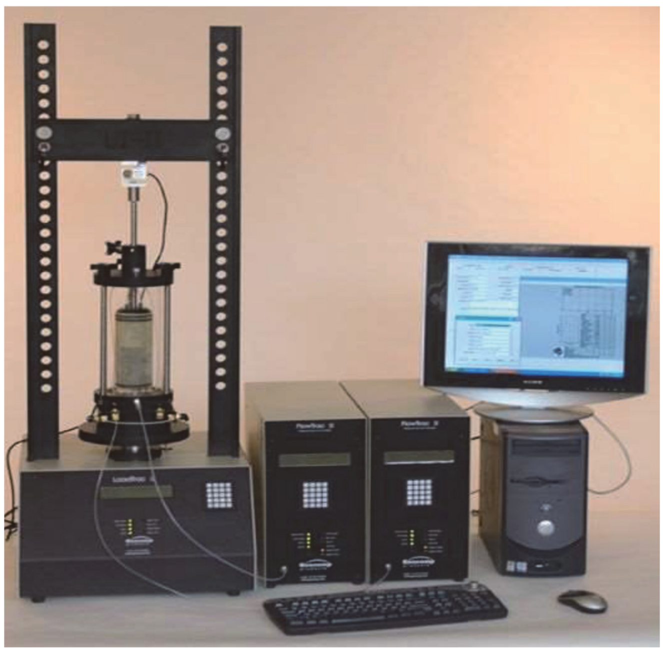

Fig. 10 The automated triaxial LoadTrac-II and FlowTrac-II System

$$q_m = \frac{\pi D_c M \varepsilon_a}{A_c} \tag{1}$$

where A_c = cross-sectional area of sample corrected after consolidation, ε_a = axial strain, D_c = diameter of the sample after consolidation and M = membrane modulus. The membrane modulus is obtained from load *vs.* strain measurement in a rubber membrane model adopting test by Greeuw *et al.* (2001).

Figure 11 presents the summary of the CIUC triaxial tests on reconstituted amorphous peat samples in the form of (a) deviatoric stress *vs.* axial strain, ε_a, (b) change in pore water pressure (Δ_u) *vs.* ε_a (c) and the plot of deviatoric stress, q *vs.* mean effective stress, p' (effective stress paths). The deviatoric and mean effective stresses at failure are respectively defined as:

$$p'_f = \frac{1}{3}(\sigma'_1 + 2\sigma'_3) \tag{2}$$

$$q_f = \sigma'_1 - \sigma'_3 \tag{3}$$

where σ'_1 and σ'_3 are the magnitudes of effective stress in the vertical and lateral direction during triaxial compression tests.

The stress-strain plot (q *vs.* ε_a), see Fig. 11(a) shows a linear elastic response for about 3% ε_a before it exhibits a strain hardening behaviour. The strain hardening behaviour tends to diminish into strain softening response between 12% to 15% axial strain for tests of higher effective stress and around 20% for 10 and 20 kPa effective stress tests. It was possible to identify peak strength for all the test relatively. There is a significant difference between the q - ε_a plot of reconstituted amorphous peat in this study and that of reconstituted peat in the literature. Hendry *et al.* (2012) observed a complete linear strain hardening response for reconstituted peat samples (fibrous peat of H2 classification) obtained from a field site in Alberta Canada, with no sign of approaching failure, even at higher effective stresses. It is clear that the effect of fibre reinforcement is significantly reduced in the peat used for this study. The additional stiffness and strength anisotropy experienced in the triaxial testing of peat depends on the fibre content and decomposition level of the peat samples (Huat *et al.* 2014).

The change in pore-water pressure, Δu plot for reconstituted amorphous peat shown in Fig. 11(b) exhibit a gradual increase of Δu at the initial stage of shearing up to about ε_a = 5%, followed by an approximately constant response to the end of the tests. At the end of the tests, the overall difference between the values of Δu and their corresponding applied cell pressure increases with an increase in cell pressure. In summary, the values of Δu appear to be lower than their corresponding applied cell pressure, which implies that the zero effective confining stress is not reached.

The stress path plots (q-p') for the 50 and 100 kPa effective stress tests (Fig. 11(c)) show an initial dilation by the increase in q with an increase in p', then followed by a decrease in p'. It can be seen that the lower effective stress tests of 10 ~ 30 kPa exhibit contractive behaviour by the gradual decrease in p' towards the end of shearing. All the samples failed without reaching the tension cut-off line (q/p' = 3), which is different from the typical characteristics of fibrous peat. The tension cut-off line in the stress path plot (q-p') denotes the condition at which cell pressure becomes zero due to the increase in excess pore water pressure of the sample. The stress path plots for the samples are all below the tension cut-off line at an axial strain of 22%. The stress path lines which does not reach towards the tension cut-off line indicate that the deviatoric stress response may be more of interparticle connection than the tension of fibres. The determined critical state of the amorphous peat is also represented by the critical state line (CSL) in the q-p' plot as shown in Fig. 11(c). The CSL is the linear fit lines obtained from the values of deviatoric stress at failure (yield stress) and the corresponding mean effective stress for each effective stress test. Although the deviatoric stress-strain response appears to bumpy towards failure (see Fig 11(a)), and the average value was considered for the CSL determination. The irregular stress-strain response towards failure is possibly as a result of the weak influence of fibre.

Figure 12 represents the relationship between the undrained shear strength and the normal effective stress for the amorphous peat samples in a Mohr-Coulomb circle plot. The line tangential to the Mohr circles represents the Mohr-Coulomb failure envelope, intercepting the vertical axis (shear stress) at 4 kPa (cohesion intercept). The effective angle of friction, ϕ' obtained from the inclined line is 33° which is in agreement with the findings of Yamaguchi *et al.* (1985) for samples tested with vertical alignments of fibres (where fibres are parallel to the major principal stress to avoid the reinforcing effect of fibre). The agreement between the value of ϕ' obtained from this study

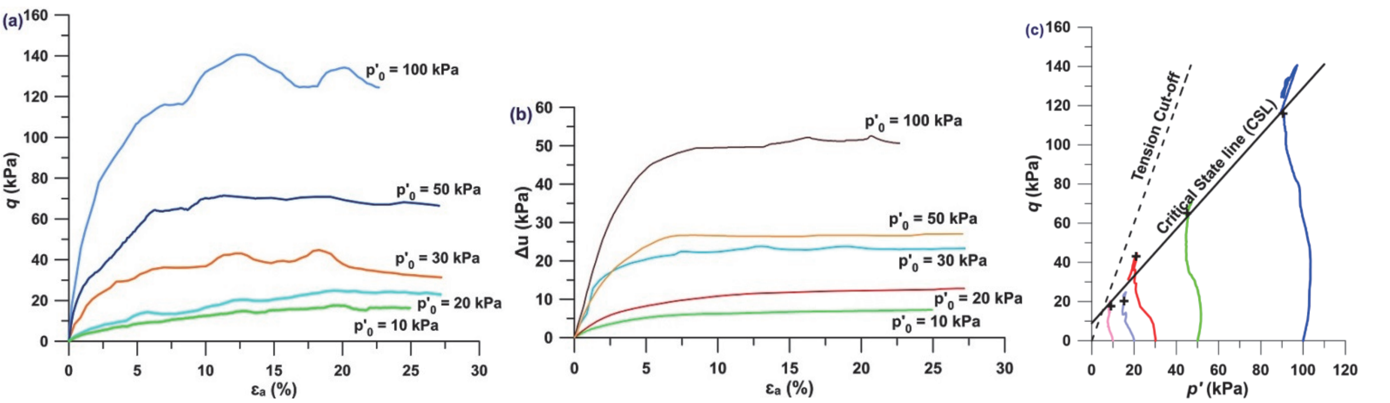

(a) Deviatoric stress *vs.* axial strain, ε_a (b) Change in pore water pressure (Δ_u) *vs.* ε_a (c) Deviatoric stress, q *vs.* mean effective stress

Fig. 11 Results from CIUC triaxial testing of reconstituted peat samples

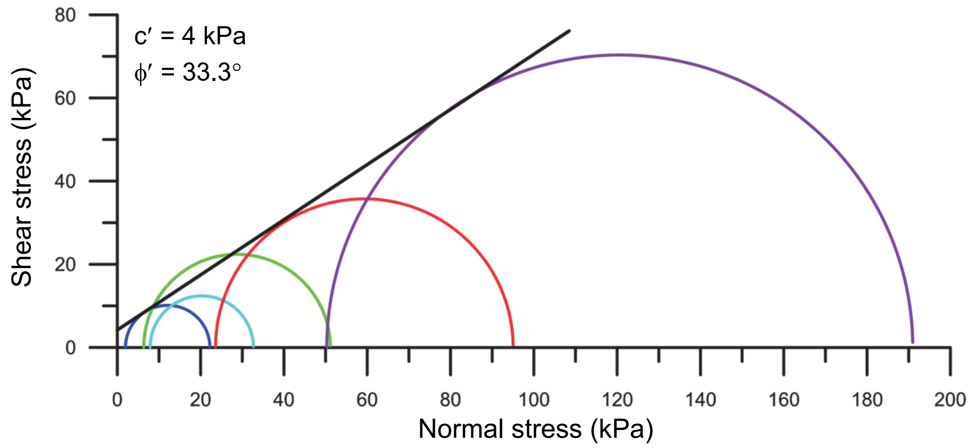

Fig. 12 Undrained shear strength *vs.* normal effective stress of amorphous peat samples

and that obtained by Yamaguchi *et al.* (1985b) shows that the effect of fibre is negligible in this present study. High friction angles within the range 50° to 85° have been reported from previous studies on undrained triaxial compression tests of peat (Den-Haan and Feddema 2012; Farrell and Hebib 1998; Hebib 2001; Yamaguchi *et al.* 1985b). Den-Haan *et al.* (1995) stated that the effective friction angles decrease with increase in density of peat.

The critical state condition at failure for the reconstituted samples tested in this study can be compared with the state of the peat at normal consolidation in the *e*-ln *p*′ plane as shown in Fig. 13. Included in the plot is the data obtained from Yang *et al.* (2016) for organic clay. Figure 13 shows linearly fitted values of void ratio after consolidation against the mean effective stress for both normally consolidated and critical state conditions. A similar linear relationship is found in the present study and the Yang *et al.* (2016) data with a slight difference in the estimated slopes. However, the amorphous peat from the present study is low in density (high void ratio) than the later. The critical state line, CSL appears not to be parallel to the normal consolidation line, NCL due to the organic nature of the particles and structural arrangement which is different from that of fine-grained soil (Budhu 2010).

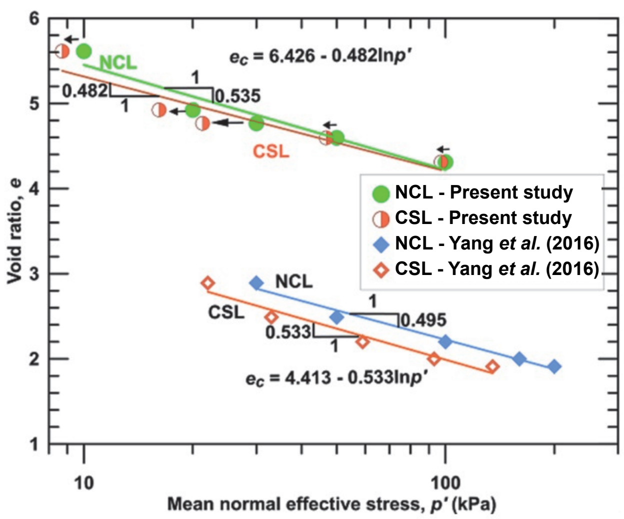

Fig. 13 Critical state (CSL) and normally consolidated (NCL) lines in *e*-ln *p*′ plane

9. CONCLUSIONS

This study involves series of various experiments conducted on highly decomposed amorphous tropical peat samples. The relationship between the microstructure, index properties, strength, compressibility and deformability properties of amorphous peat is explored to understand the engineering behaviour of amorphous tropical peat. The outcome of the experimental work is summarised below:

1. The index properties of the amorphous peat indicate that the peat is dominated by organic contents that are highly decomposed. The humification process has led to the relative increase in specific gravity and reduction in water content. The measured index properties are relatively stable.
2. The microstructure reveals that the peat morphology is more of compact amorphous-granular particles with no physical evidence of hollow cellular connections or fibre entanglement. Higher magnified views reveal homogeneous non-crystalline micro-particles that are colloidal in structure. Traces of some solid sheet-like structure are also found. Though the studied peat is made of about 94% organic content, the SEM images hardly show evidence of plant-derived microparticles.
3. The tested amorphous peat displayed high initial void ratio and compressibility characteristics. Comparison of the compressibility behaviour of reconstituted and undisturbed samples suggests less significant structural anisotropy. The average compression index, C_c for the reconstituted and undisturbed tests are 4.35 and 5.37 respectively and the average ratio of C_α / C_c measured in this study is 0.05. The similar compressibility and deformability characteristics of both reconstituted and undisturbed sample in the one-dimensional compression tests can be linked to the insignificant effect of fibre that has been decomposed.
4. The stress path of amorphous peat samples did not touch the tension cutoff line throughout the triaxial test, which is due to significantly low fibre content. The samples were able to achieve a relative peak failure at higher strains, and the pore water pressure generated at the end of each test is lower than their corresponding applied cell pressure. The subsidence of the strain hardening effect is evidence of high decomposition of the fibre. The angle of friction (33°) estimated from this study is relatively low as compared to fibrous peat.

5. The comparison of the critical state condition at failure with the state of the peat at normal consolidation in the e-ln p' plane exhibit a typical stress path for normally consolidated undrained soils.

This study demonstrated that the complexities in the laboratory test of peat, especially triaxial testing are less significant in amorphous peat and laboratory strength estimation can be reliable for amorphous peat.

ACKNOWLEDGEMENTS

The work presented in this paper is supported by the UNIMAS small Grant Scheme (grant No. FO2(S165)/1198/2015(02)) and the Fundamental Research Grant Scheme (Grant No. FRGS/TK01(02)/1302/2015(19)). The first author acknowledges the guidance of Professor Amir Azam Khan of the Department of Mechanical and Manufacturing Engineering, UNIMAS on the use of SEM.

REFERENCES

Al-ani, H., Erwin, O., and Gary, C. (2013). "Engineering properties of peat in estuarine environment." *Proceedings of Foundation and Soft Ground Engineering Challenges ICTDMU-1*, Mekong Delta, 181-193.

Amuda, A.G., Fauzan, S., Alsidqi, H., Siti Noor Linda, T., Noel, B., and Aliaa, M. (2019). "Measurement of amorphous peat shear strength in the direct shear box at high displacement rates." *Geotechnical and Geological Engineering*, **37**(2), 1059-1072. http://doi.org/10.1007/s10706-018-0643-3

ASTM D1587 (2015). *Standard Practice for Thin-Walled Tube Sampling of Fine-Grained Soils for Geotechnical Purposes. ASTM Book of Standards*. West Conshohocken, PA. http://doi.org/10.1520/D1587_D1587M-15

ASTM D1997 (2013). *Standard Test Method for Laboratory Determination of the Fiber Content of Peat Samples by Dry Mass. ASTM Book of Standards*. Vol. 04.08. West Conshohocken, PA: ASTM International. http://doi.org/10.1520/D1997

ASTM D2487 (2011). *Standard Practice for Classification of Soils for Engineering Purposes (Unified Soil Classification System). ASTM Standard Guide*. http://doi.org/10.1520/D2487-11

ASTM D2974 (2014). *Standard Test Methods for Moisture, Ash, and Organic Matter of Peat and Organic Soils Significance*: West Conshohocken, PA: ASTM International. http://doi.org/10.1520/D2974-14.obtaining

ASTM D4427 (2002). *Standard Classification of Peat Samples by Laboratory Testing*. American Society of Testings and Methods, ASTM. http://doi.org/10.1520/D4427-13.2

ASTM D4767 (2011). *Standard Test Method for Consolidated Undrained Triaxial Compression Test for Cohesive Soils*. ASTM International. http://doi.org/10.1520/D4767-11

ASTM D854 (2010). *Standard Test Methods for Specific Gravity of Soil Solids by Water Pycnometer. ASTM International Standard Methods*. West Conshohocken, PA: ASTM International. http://doi.org/10.1520/D0854-10

Boelter, D.H. (1968). "Important physical properties of peat materials." *Proceedings of Third International Peat Congress*, Quebec, Canada, 150-154. http://doi.org/10.1.1.628.9973

Boylan, N., Long, M., and Mathijssen, F.A.J.M. (2011). "In situ strength characterisation of peat and organic soil using full-flow penetrometers." *Canadian Geotechnical Journal*, **48**(7), 1085-1099. http://doi.org/10.1139/t11-023

Boylan, N. (2008). *The Shear Strength of Peat*. Ph.D. Dissertation, University College Dublin.

Budhu, M. (2010). *Soil Mechanics and Foundations*. 3rd Ed., John Wiley & Sons, Inc. http://doi.org/10.0470556846

Cola, S. and Giampaolo, C. (2005). "The shear strength behavior of two peaty soils." *Geotechnical and Geological Engineering*, **23**(6), 679-695. http://doi.org/10.1007/s10706-004-9223-9

DenHaan, E.J. and Kruse. G.A.M. (2007). "Characterisation and Engineering Properties of Dutch Peats." *Proceedings of Characterisation and Engineering Properties of Natural Soils*, Singapore: Taylor and Francis, 2101-2133. http://doi.org/10.1016/j.jada.2008.10.064

DenHaan, E.J., Uriel, A.O., and Rafnsson. E.A. (1995). "Special Problem Soils/Soft Rocks." *Proceedings of the 11th European Conference on Soil Mechanics and Foundation Engineering-Theme*, Copenhagen, Denmark, Danish Geotechnical Society, **7**, 139-180. http://doi.org/8789833007

DenHaan, E.J. and Feddema, A. (2013). "Deformation and Strength of Embankments on Soft Dutch Soil." *Proceedings of the Institution of Civil Engineers — Geotechnical Engineering*, **166**(3), 239-252. http://doi.org/10.1680/geng.9.00086

Edil, T.B. and Wang. X. (2000). "Shear Strength and Ko of Peats and Organic Soils." *Geotechnics of High Water Content Materials, ASTM STP 1374*, West Conshohocken: ASTM, Edil, T.B. and Fox, P., Eds., 209-225. http://doi.org/10.1520/STP14369S

Farrell, E.R. and Hebib, S. (1998). "The Determination of Geotechnical Parameters of Organic Soils." *Proceedings of an International Symposium on Problematic Soils*, Sendai, Japan: Balkema, Rotterdam, **1**, 33-36.

Fredriksson, D. (1996). "Peat Resources in Sweden." *Global Peat Resources*. 137-144.

Grognet, M. (2011). *The Boundary Conditions in Direct Simple Shear Tests*. M.Sc Thesis, Delft University of Technology. http://doi.org/uuid:c320f947-6a68-4e8b-830a-b94b88d3e43f

Guzman, E.M.B.D. and Alfaro, M.C. (2018). "Laboratory-Scale Model Studies on Corduroy-Reinforced Road Embankments on Peat Foundations Using Transparent Soil." *Transportation Geotechnics*, **16**, 1-10. http://doi.org/10.1016/j.trgeo.2018.05.002

Habib-Musa, M. (2015). *Post Cyclic Behaviour of Malaysian Peat Soil*. MEng Thesis, Universiti Tun Hussein Onn Malaysia.

Hanrahan, E.T. (1954). "An Investigation of Some Physical Properties of Peat." *Géotechnique*, **4**(3), 108-123.

Hayashi, H., Nobutaka, Y., Toshiyuki, M., Hiroyuki, T., and Satoshi, N. (2012). "Coefficient of Earth Pressure at Rest for Normally and Overconsolidated Peat Ground in Hokkaido Area." *Soils and Foundations*, **52**(2), 299-311. http://doi.org/10.1016/j.sandf.2012.02.007

Hebib, S. (2001). *Experimental Investigation on the Stabilization of Irish Peat*. Ph.D. Dissertation, University of Dublin, Trinity College.

Hendry, M.T., Sharma, J.S., Martin, C.D., and Barbour, S.L. (2012). "Effect of fibre content and structure on anisotropic elastic stiffness and shear strength of peat." *Canadian Geotechnical Journal*, **49**(4), 403-415. http://doi.org/10.1139/t2012-003

Hobbs, N.B. (1986). "Mire morphology and the properties and behaviour of some British and foreign peats." *Quarterly Journal of Engineering Geology and Hydrogeology*, **19**(1), 7-80. http://doi.org/10.1144/GSL.QJEG.1986.019.01.02

Huat, B.B.K., Arun, P., Afshin, A., and Sina, K. (2014). *Geotechnics of Organic Soils and Peat. Geotechnics of Organic Soils and Peat*. 1st Ed., London: Taylor and Francis. http://doi.org/10.1201/b15627

Huat, B.B.K, Sina, K., Arun, P., and Maassoumeh, B. (2011). "State of an art review of peat: General perspective." *International Journal of the Physical Sciences*, **6**(8), 1988-1996.

http://doi.org/10.5897/IJPS11.192

Huat, B.B.K., Shukri, M., Teori, K., and Ubah, B. (2003). *Organic and Peat Soil Engineering*. Universiti Putra Malaysia Press.

Joosten, H. (2015). "Changing paradigms in the history of tropical peatland research." *Tropical Peatland Ecosystems*, 33-48. Tokyo: Springer. http://doi.org/10.1007/978-4-431-55681-7_2

Kazemian, S. and Hossien, M. (2013). "Effect of cement-sodium silicate grout on the compressibility parameters of fibrous peat." *Advanced Materials Research*, Oakland, Califonia: ASCE, **629**, 461-465. http://doi.org/10.4028/www.scientific.net/AMR.629.461

Landva, A. (2006). "Characterization of escuminac peat and construction on peatland." *Characterisation and Engineering Properties of Natural Soils*, Singapore: Taylor and Francis, 2135-2191. http://doi.org/10.1201/NOE0415426916.ch14

Landva, A.O. and Pheeney, P.E.. (1980). "Peat fabric and structure." *Canadian Geotechnical Journal*, **17**(3), 416-435. http://doi.org/10.1139/t80-048

Landva, A.O. and La Rochelle. P. (1983). "Compressibility and shear characteristics of radforth peats." *Testing of Peats and Organic Soils*, P. M. Jarrett, Ed., West Conshohocken, PA: ASTM International, 157-191. http://doi.org/10.1520/STP37341S

Lee, J.-S., Sun, Y.S., and Lee, C.H. (2015). "Geotechnical and geophysical characteristics of muskeg samples from Alberta, Canada." *Engineering Geology*, **195**, 135-141. http://doi.org/10.1016/j.enggeo.2015.04.030

Long, M. (2005). "Review of peat strength, peat characterisation and constitutive modelling of peat with reference to landslides." *Studia Geotechnica et Mechanica*, **27**(3-4), 67-90. http://doi.org/10.1.1.1017.9028&rep=rep1&type=pdf

Mesri, G. and Ajlouni. M. (2007). "Engineering properties of fibrous peats." *Journal of Geotechnical and Geoenvironmental Engineering*, ASCE, **133**(7), 850-866. http://doi.org/10.1061/(ASCE)1090-0241(2007)133:7(850)

O'Kelly, B.C. (2015). "Effective stress strength testing of peat." *Environmental Geotechnics*, **2**(1), 34-44. http://doi.org/10.1680/envgeo.13.00112

Pichan, S. and O'Kelly, B.C. (2012). "Effect of decomposition on the compressibility of fibrous peat." *Proceedings of GeoCongress 2012*, Reston, VA: American Society of Civil Engineers, **8**, 4329-4338. http://doi.org/10.1061/9780784412121.445

Santagata, M., Bobet, A., Johnston, C.T., and Hwang. J.H. (2008). "One-dimensional compression behavior of a soil with high organic matter content." *Journal of Geotechnical and Geoenvironmental Engineering*, ASCE, **134**, 1-13. http://doi.org/10.1061/(ASCE)1090-0241(2008)134:1(1)

Tie, Y.L.K. and Hong, S.K. (1979). *A Review of Lowland Organic Soils of Sarawak*. Department of Agriculture, Technical Paper 4, Research Branch, Sarawak, Kuching, Malaysia.

Wetlands International (2010). *A Quick Scan of Peatlands in Malaysia*. Wetlands International, Malaysia: Petaling Jaya, Malaysia.

Wösten, J.H.M., Ismail, A.B., and Van Wijk, A.L.M. (1997). "Peat subsidence and its practical implications: A case study in malaysia." *Geoderma*, **78**(1-2), 25-36. http://doi.org/10.1016/S0016-7061(97)00013-X

Yamaguchi, H., Ohira, Y., and Kogure. K. (1986). "Volume change characteristics of undisturbed fibrous peat." *International Journal of Rock Mechanics and Mining Sciences & Geomechanics Abstracts*, **23**(1), A12. http://doi.org/10.1016/0148-9062(86)91763-8

Yamaguchi, H.Y., Yoshinori, O., Keiji, K., and Shigeru, M. (1985). "Undrained shear characteristics of normally consolidated peat under triaxial compression and extension conditions." *Soils and Foundations*, **25**(3), 1-18. http://doi.org/10.3208/sandf1972.25.3_1

Yang, Z.X., Zhao, C.F., Xu, C.J., Wilkinson, S.P., Cai, Y.Q., and Pan, K. (2016). "Modelling the engineering behaviour of fibrous peat formed due to rapid anthropogenic terrestrialization in Hangzhou, China." *Engineering Geology*, **215**, 25-35.

Zainorabidin, A. and Wijeyesekera. D.C. (2007). "Geotechnical challenges with malaysian peat." *Proceedings of Advances in Computing and Technology 2nd Annual Conference*, Docklands London: University of East London, 252-261. http://doi.org/10.1016/j.jada.2010.08.016

Zhang, Lin and O'kelly, B.C. (2013). "Constitutive models for peat — A review." *Proceedings of 12th International Conference on Computational Plasticity – Fundamentals and Applications (COMPLAS XII)*, Barcelona, Spain: International Center for Numerical Methods in Engineering (CIMNE), 1294-1304.

Zulkifley, M.T.M., Ng, T.F., Abdullah, W.H., Raj, J.K., Shuib, M.K., Ghani, A.A., and Ashraf, M.A. (2015). "Geochemical characteristics of a tropical lowland peat dome in the Kota Samarahan-Asajaya area, West Sarawak, Malaysia." *Environmental Earth Sciences*, **73**(4), 1443-1458. http://doi.org/10.1007/s12665-014-3504-2

Zulkifley, M.T.M., Ng, T.F., Raj, J.K., Hashim, R., Ghani, A., Shuib, M.K., and Ashraf, M.A. (2013). "Definitions and engineering classifications of tropical lowland peats." *Bulletin of Engineering Geology and the Environment*, **72**(3-4), 547-553. http://doi.org/10.1007/s10064-013-0520-5

Zwanenburg, C., Den Haan, E.J., Kruse, G.A.M., and Koelewijn, A.R. (2012). "Failure of a trial embankment on peat in Booneschans, the Netherlands." *Géotechnique*, **62**(6), 479-490. http://doi.org/10.1680/geot.9.P.094

Zwanenburg, C. and Jardine. R.J. (2015). "Laboratory, in situ and full-scale load tests to assess flood embankment stability on peat." *Géotechnique*, **65**(4), 309-326. http://doi.org/10.1680/geot.14.P.257